

Electronic Supplementary Information for

**Aggregation of CeO₂ particles with aligned grains drives
sintering of Pt single atoms in Pt/CeO₂ catalysts**

Jaeha Lee^{1,4Δ}, Sungsu Kang^{1,2Δ}, Eunwon Lee¹, Minho Kang^{1,2}, Jongbaek Sung^{1,2}

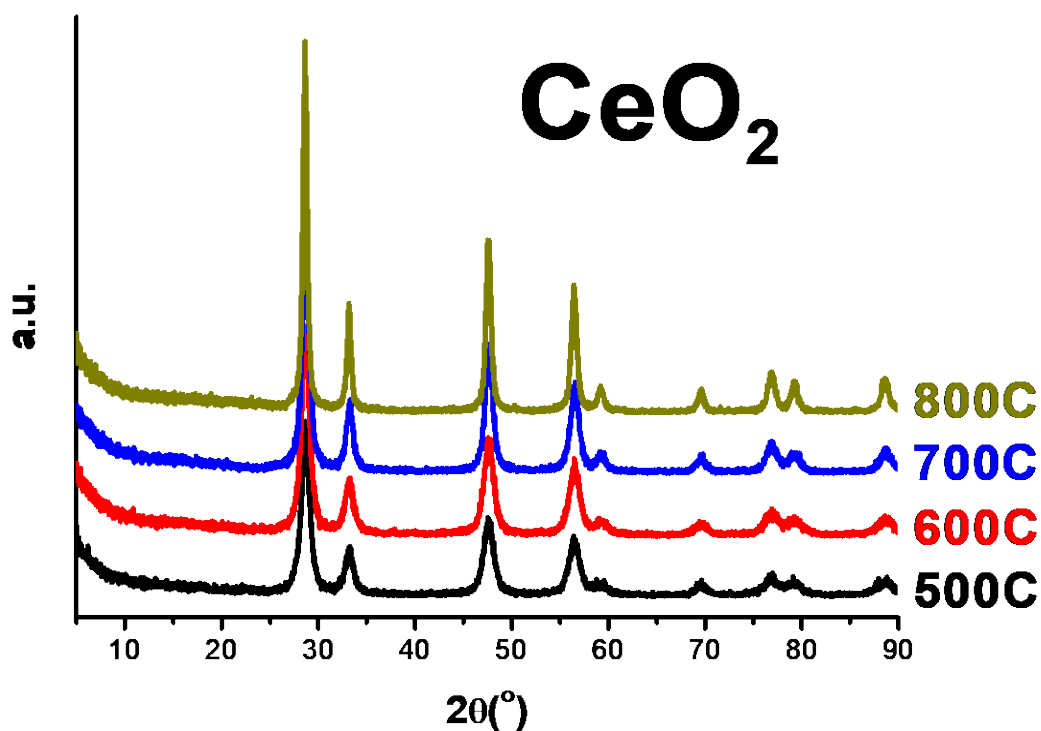
Tae Jin Kim³, Phillip Christopher⁴, Jungwon Park^{1,2*}, Do Heui Kim^{1*}

¹ School of Chemical and Biological Engineering, Institute of Chemical Processes, Seoul National University, Seoul 08826, Republic of Korea

² Center for Nanoparticle Research, Institute for Basic Science (IBS), Seoul 08826, Republic of Korea

³ Department of Materials Science and Chemical Engineering, Stony Brook University, Stony Brook, New York 11794, United States

⁴ Department of Chemical Engineering, University of California Santa Barbara, Santa Barbara, California 93106, United States



CeO₂

Oxidation temperature	BET surface area (m ² /g)	Crystalline size (nm)
500 °C	129	8.6
600 °C	118	8.6
700 °C	101	11.2
800 °C	65	17.2

Fig. S1. (top) XRD patterns of CeO₂ after oxidation at 500, 600, 700, and 800 °C for 2 h. (bottom) BET surface area calculated from N₂ adsorption isotherm, and crystalline size of CeO₂ calculated from XRD patterns by using Scherrer equation.

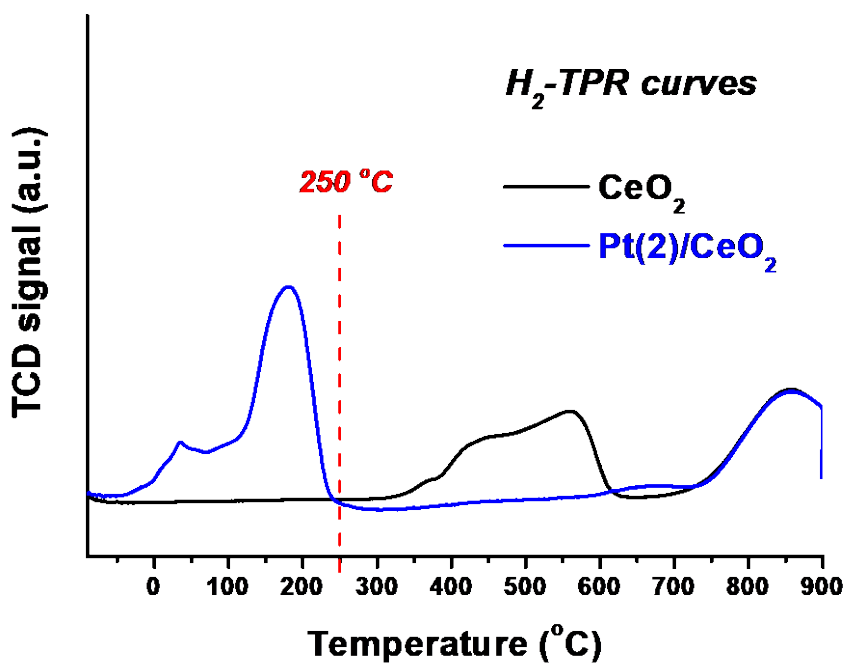


Fig. S2 H₂-TPR curve of CeO₂ 500C and Pt/CeO₂ 500C. The reduction of Pt/CeO₂ surface is completed at temperature lower than 250 °C while the reduction of bulk oxygen occurs at temperature higher than 600 °C. Thus, we conducted 250R treatment to selectively remove surface oxygen in Pt/CeO₂ 500C before high-temperature thermal treatment.

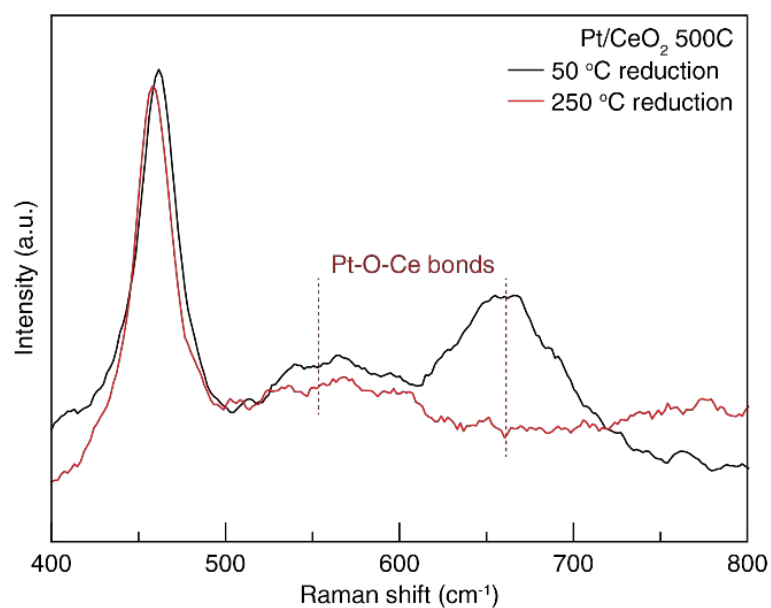


Fig. S3. *In-situ* Raman spectra of Pt/CeO₂ 500C collected after the H₂ treatment at 50 °C (black line) and 250 °C (red line). Raman shifts from Pt-O-Ce bond are marked in the figure.

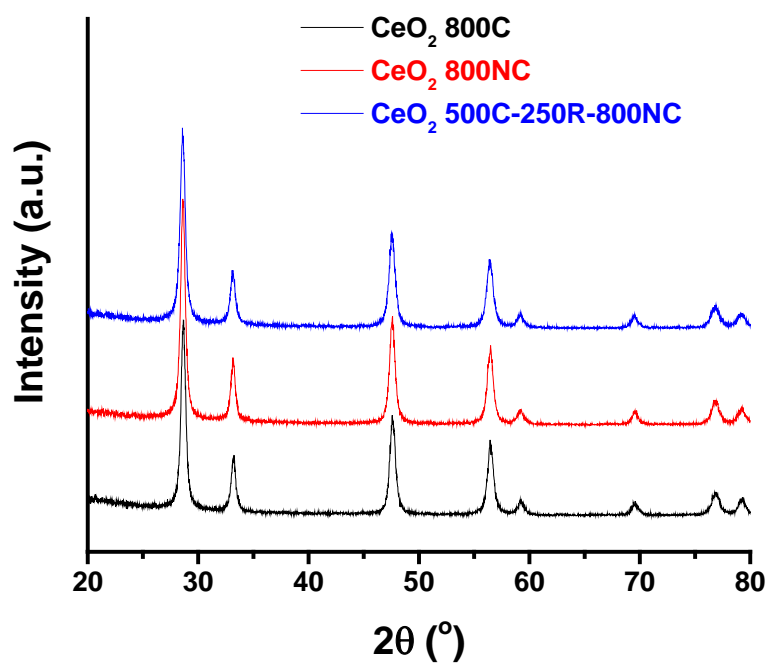


Fig. S4. XRD patterns of CeO₂ 800C, 800NC and 500C-250R-800NC samples.

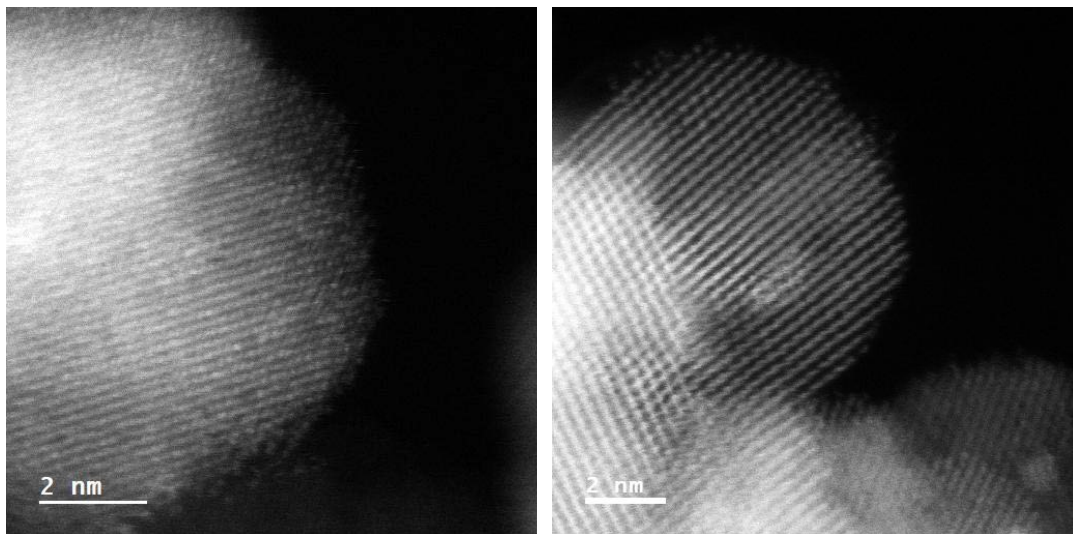


Fig. S5 Representative HAADF-STEM images of Pt/CeO₂ 500C-250R. At 2 wt% of Pt loading, both Pt SA and Pt NP were found on Pt/CeO₂ 500C-250R. However, the number density of Pt NP was low on TEM images (e.g. less than 1 Pt NP per CeO₂ particle). The Pt NP formation could be further suppressed by decreasing the Pt loading (data not shown). However, the number density of Pt SA also decreases, making it difficult to study the correlation between Pt sintering and CeO₂ aggregation as in Figure 2 or 3.

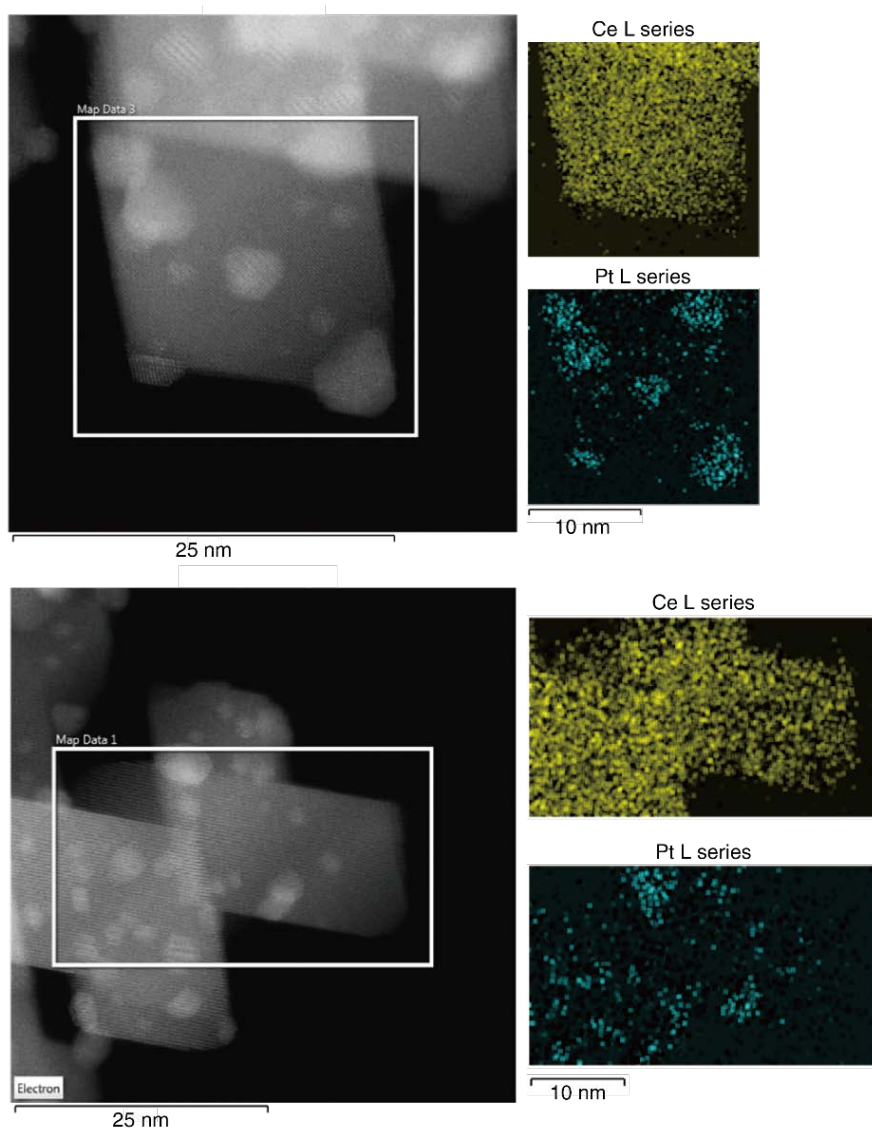


Fig. S6 HAADF-STEM images of Pt/CeO₂ 500C-250R-800NC and the corresponding EDS elemental maps of boxed regions in the HAADF-STEM images. The EDS elemental maps clearly show that the Pt NPs are formed in Pt/CeO₂ 500C-250R-800NC.

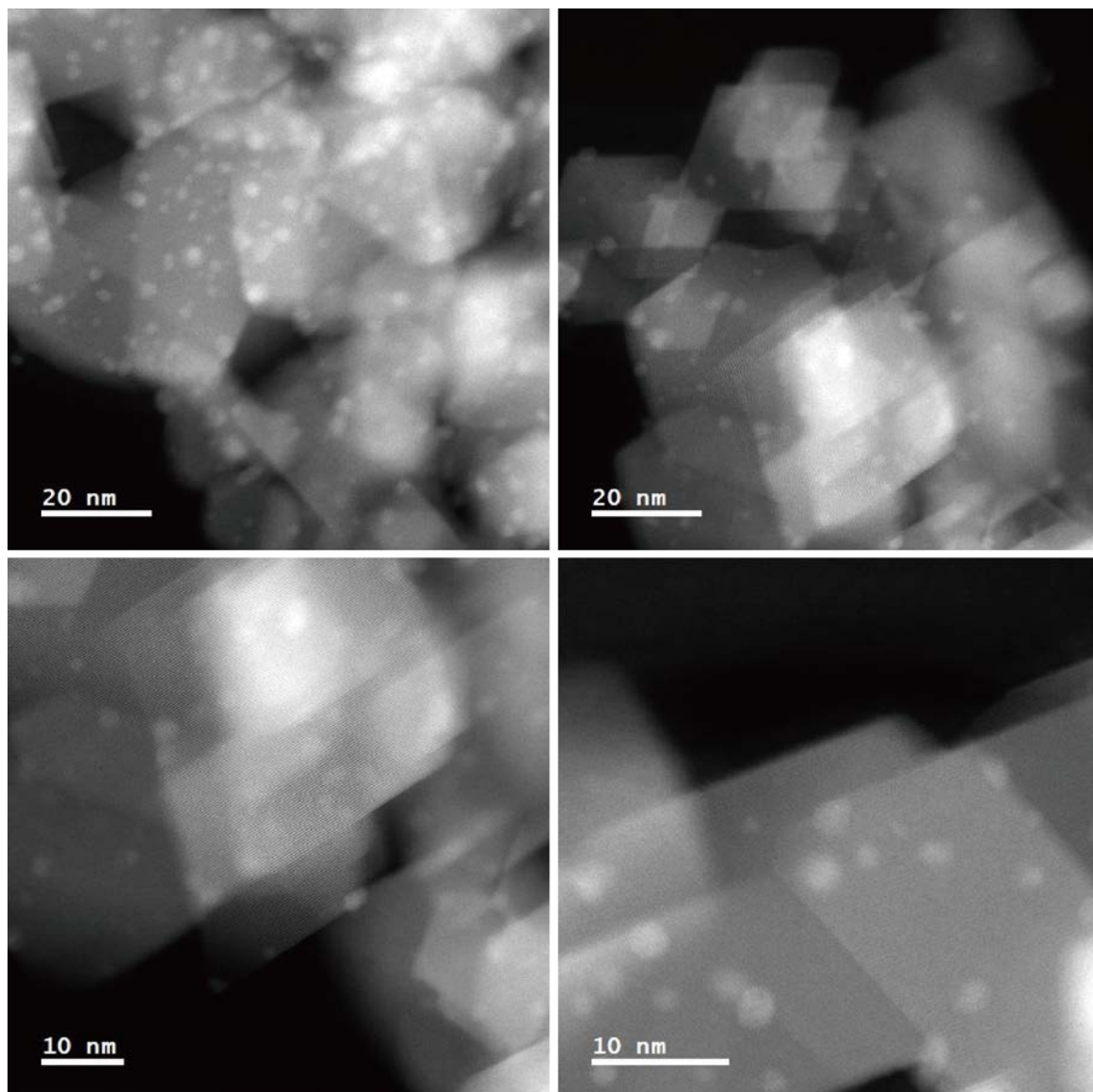


Fig. S7 Representative HAADF-STEM images of Pt/CeO₂ 500C-250R-800NC.

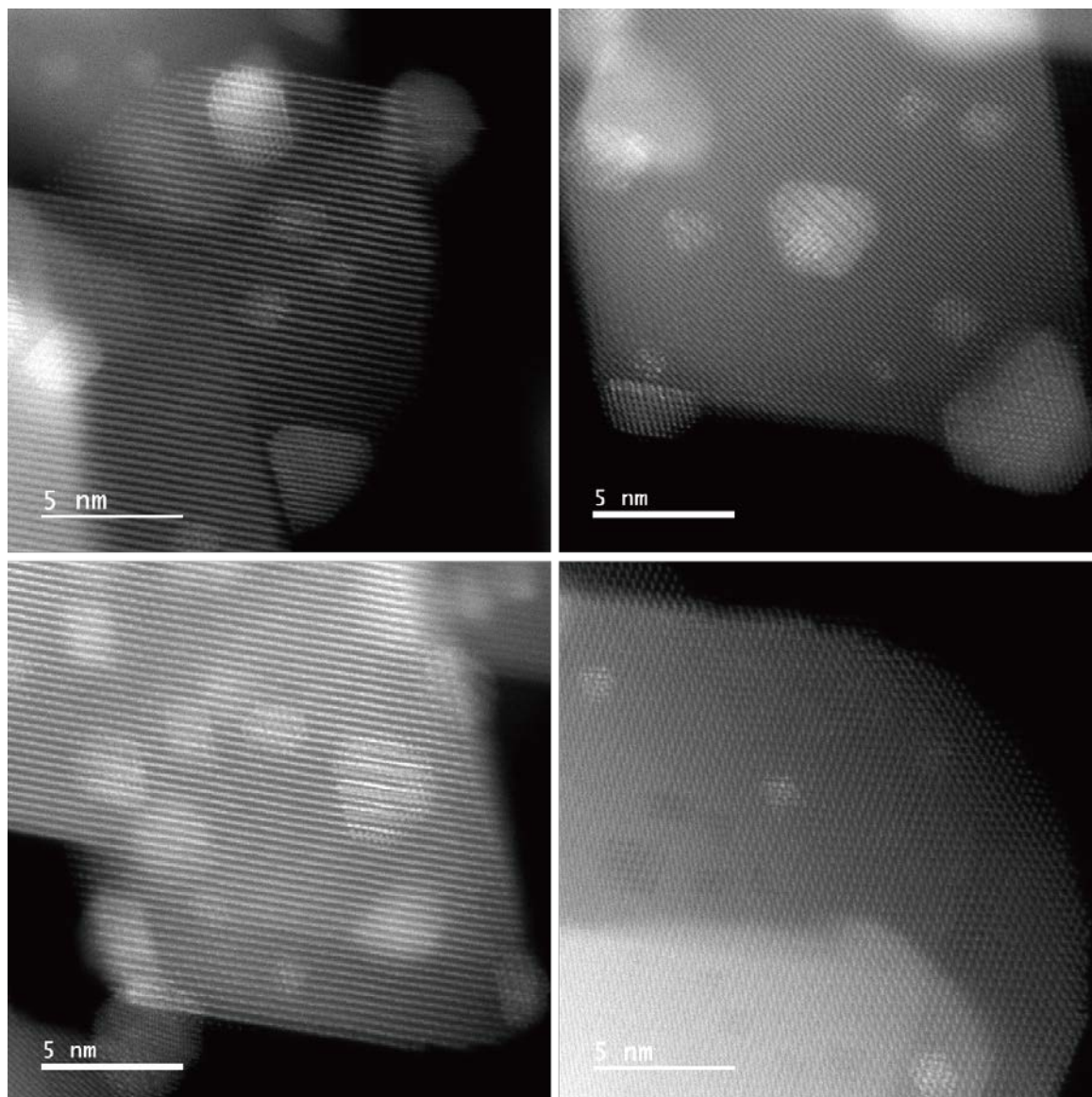


Fig. S8 Representative HAADF-STEM images of Pt/CeO₂ 500C-250R-800NC at atomic resolution. While abundant of Pt NPs (>1 nm) are found, Pt SA is barely observed.

Supplementary Discussion I: Using silicon nitride TEM grids for *ex-situ* heating and imaging of Pt/CeO₂ particles on the grid

Understanding aggregation behavior of support particles during a thermal treatment requires control over the density of CeO₂ particles at a single-particle scale. Calcination of catalysts is usually conducted in a reactor filled with dense powders of the CeO₂ particles. The high density of the catalyst particles induces aggregation of CeO₂ particles into single-crystalline particles with octahedral shapes after the thermal treatment. Within the larger CeO₂ particles formed after the calcination, we cannot see the morphology of untreated CeO₂ particles or the domain boundaries between them, and discriminating individual CeO₂ particles in the aggregates is challenging. Thus, understanding how the thermal behavior of the support particles affects the catalytic system requires control over the degree of support aggregation, which can be achieved by spatially distributing Pt/CeO₂ particles on a substrate.

We spatially separated Pt/CeO₂ particles by dispersing the powders of Pt/CeO₂ 500C-250R particles in ethanol, and placing a drop of the dispersion onto a silicon nitride (SiN_x) TEM grid, which endures the thermal treatment at 800 °C and can be directly used for a TEM observation without further handling. The fabrication of SiN_x TEM grids is described elsewhere¹; briefly, 25-nm-thick low-stress SiN_x was deposited on both side of a 4-inch silicon (Si) wafer (p-type, double side polished, 100 mm-thick) by low pressure chemical vaporized deposition at 800 °C (LEAD Engineering Co., VULCAN-H62RL, Korea). Lithographic patterning and etching procedures were performed to fabricate the TEM grids with SiN_x windows. Hexamethyldisizazne (HMDS, Sigma Aldrich, USA) was spin coated on one side of the wafer with the spin coater (ACE-200, Dong Ah Trade Corp., Korea) at the 3000 rpm for 30 s and the wafer was baked at 95 °C for 30 s. Positive photoresist (PR, AZ 5214 E, Duksan Hichem, Korea) was spin coated on the same side of the wafer with the same condition and the wafer was baked

at 110 °C for 50 s. Ultraviolet light was selectively exposed to the spin-coated PR with mask aligner (MDA-600S, MIDAS SYSTEM, Korea) and the PR was patterned by immersing the wafer in the developer (AZ 300 MIF, Merck, Germany) for 1 min and rinsed with DI water. SiN_x layer was selectively dry etched with reactive ion etching process with sulfur hexafluoride (SF₆) gas at 3 sccm and RF power of 50 W in 100 mTorr. The PR was subsequently eliminated by immersing the wafer in acetone for 30 min and rinsed with DI water. Si was wet etched in 8 % (w/w) potassium hydroxide (KOH, Daejung, Korea) solution at 85 °C until window area remained with freestanding SiN_x membrane. After the etching process fabricated TEM devices were rinsed with DI water to eliminate residues formed during the wet etching process. The fabricated SiN_x TEM grid has a suspended SiN_x windows with the thickness of ~25 nm (Fig. S9), enabling the observation of atoms in the thermal-treated Pt/CeO₂ particles. Typical TEM grids having a thin amorphous carbon film on a Cu mesh cannot endure the thermal treatment performed at 800 °C; the carbon film is detached from the metal mesh due to large difference in the thermal expansion coefficient between amorphous carbon and Cu, and relatively weak adherence of the carbon film to the Cu mesh.

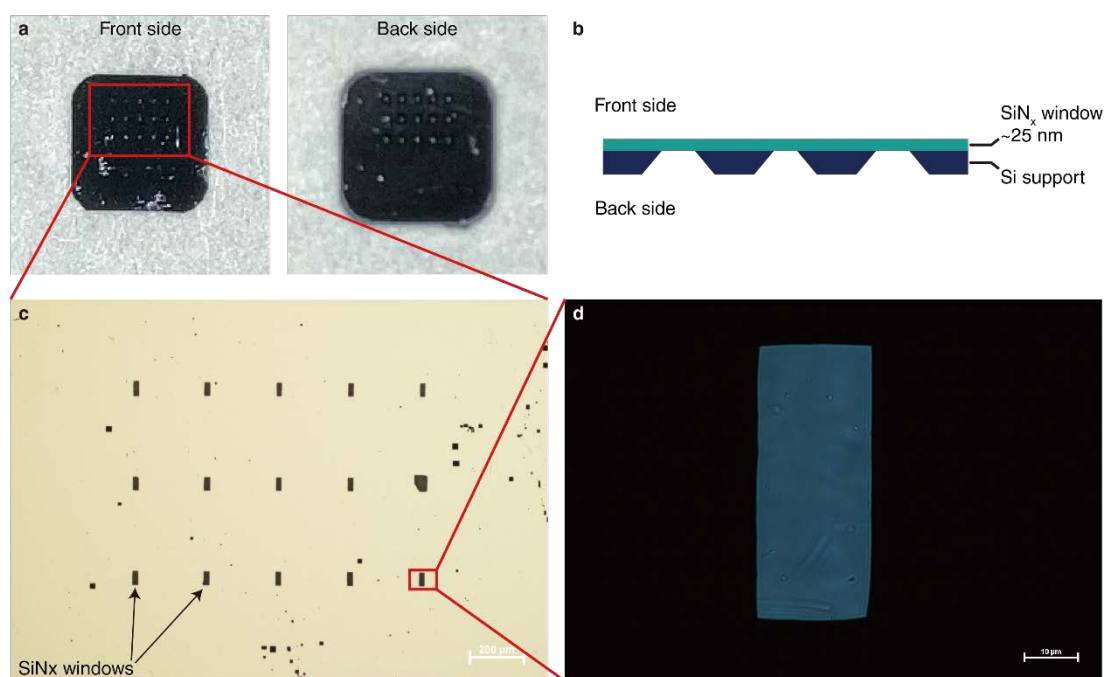


Fig. S9 Structures of SiN_x TEM grids used to spatially distributed Pt/CeO₂ particles. (a) Overall view of a SiN_x TEM chip, showing the front side (left) and the back side (right). (b) Illustration showing the side view of the chip. (c) Enlarged view of the center of the SiN_x chip (marked with red in (a)), showing SiN_x windows that appear as black squares. (d) Enlarged view of a SiN_x window. The SiN_x membrane can withstand the 800NC treatment.

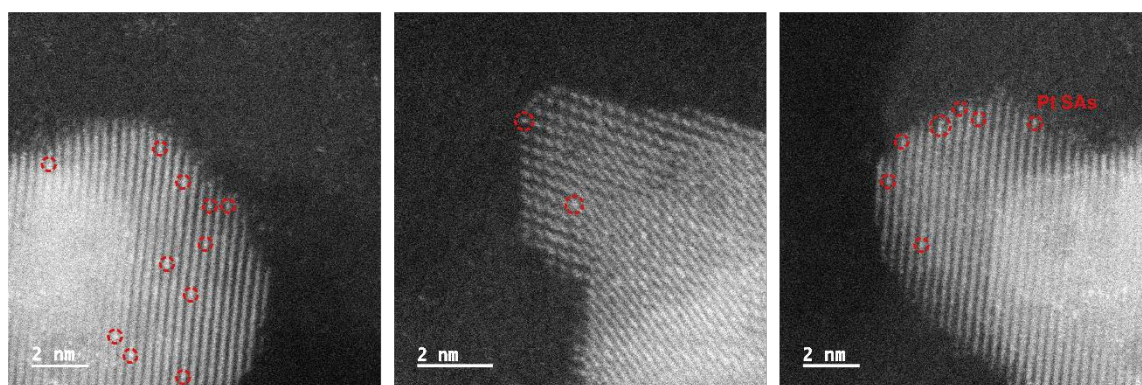


Fig. S10 HAADF-STEM images of Pt SAs in the isolated Pt/CeO₂ particles on SiN_x TEM grid. The Pt SAs are marked with red circles in the images.

Supplementary Discussion II: *In-situ* TEM of Pt/CeO₂

High-temperature thermal treatment of 800NC on Pt/CeO₂ 500C-250R induces both the aggregation of CeO₂ support particles and the sintering of Pt SAs. Although the presented *ex-situ* XRD, TEM, and HAADF-STEM analyses reveal the presence of Pt SAs before the thermal treatment and the absence of Pt SAs after the thermal treatment, it cannot provide the detailed information on sintering processes and chemical environment at the moment of Pt NP formation. To identify whether or how the sintering of Pt and the aggregation of CeO₂ is correlated by real-time observations, we exploited *in-situ* heating TEM of Pt/CeO₂.

Samples for *in-situ* TEM experiments were prepared by placing a drop of Pt/CeO₂ 500C-250R dispersed in ethanol on a heating chip (Nano-Chip) by DENSsolutions, and drying overnight. As shown in Fig. S11, the heating chip has electron-transparent windows which are made of a SiN_x membrane with approximated thickness of 50 nm. The thin SiN_x membrane provides the resolution sufficient to observe Pt NPs as small as about 1 nm. For TEM observations, JEOL JEM-2100F (scanning) transmission electron microscope operated at 200 kV and equipped with a Schottky field emission gun and a Gatan Ultrascan 1000XP charge-couple device (CCD) camera was used. The heating chip was loaded on a DENSsolutions Wildfire holder, and subsequently the holder was inserted into the TEM column. The specimen was first heated to the target temperature at rate of 50 °C/min under vacuum condition. When the temperature reached the desired temperatures (600, 700, or 800 °C), the heating was paused and TEM images are acquired at the selected temperature.

We observed that prolonged electron beam irradiation to the Pt/CeO₂ 500C-250R suppress the sintering of Pt and the aggregation of CeO₂ particles even at elevated temperature of 800 °C, as shown in Fig. S12. This is presumably because high-energy electrons may change the surface structure of CeO₂, leading to the formation of Pt-O-Ce bonds between Pt atoms on the CeO₂

surface and O atoms originally present in a sub-surface region. Therefore, during the entire imaging process, we minimized the time that the samples are exposed to the electrons by blanking the electron beam except when focusing and acquiring the images. It should be noted that the vacuum environment in the TEM column may result in different thermal behavior from the 800NC treatment with N₂ gas environment. However, the observed thermal behavior was similar between samples treated under vacuum environment or N₂ environment; the size of sintered Pt NPs is measured to be 2-5 nm for both samples, and the CeO₂ crystallites are coherently aggregated after the high-temperature treatment. These results suggest that the observed thermal behavior of Pt/CeO₂ 500C-250R might be irrelevant to the gas environment during heating.

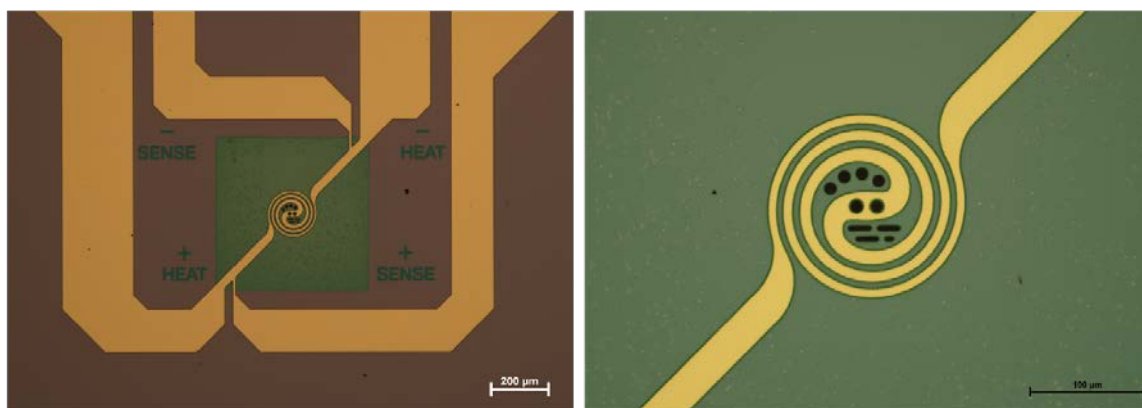


Fig. S11 Heating chip used for *in-situ* TEM of Pt/CeO₂ 500C-250R. (left) Overall view of the heating chip. The center region is heated via Joule heating of an orange-colored metal spiral. (right) Enlarged view of the viewing windows (black-colored regions).

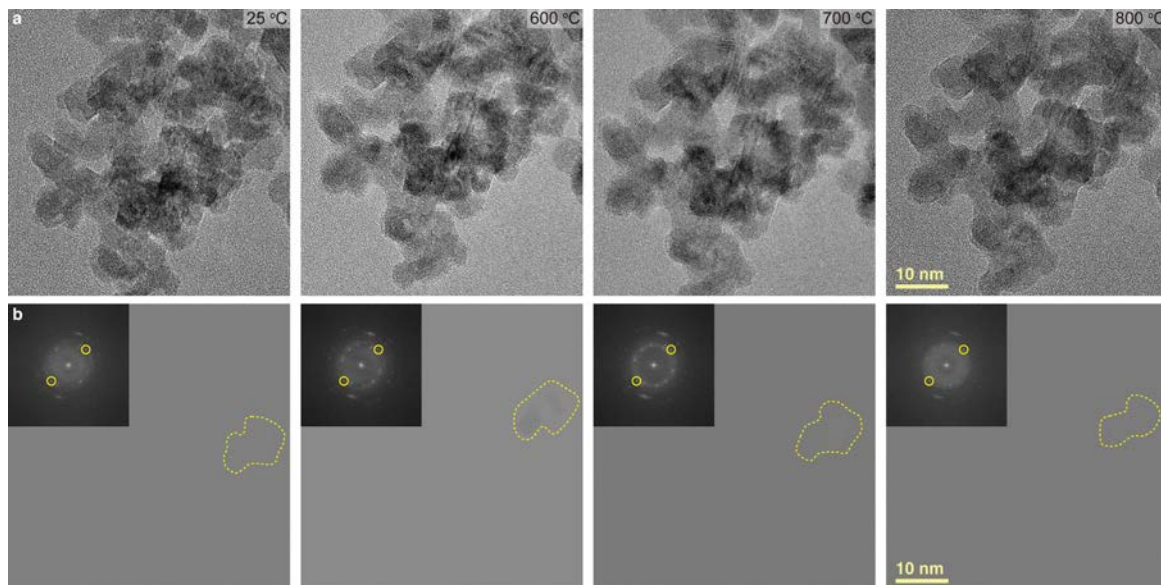


Fig. S12 *In-situ* heating TEM of Pt/CeO₂ 500C-250R during continuous electron beam irradiation. (a) TEM images of Pt/CeO₂ 500C-250R during *in-situ* heating (upper panels), and inverse Fourier transforms (lower panels) showing a CeO₂ domain selected from the Fourier transforms of the TEM images (marked with circles in the inset images). Here, the electron beam was continuously irradiated to the sample during the *in-situ* TEM observation.

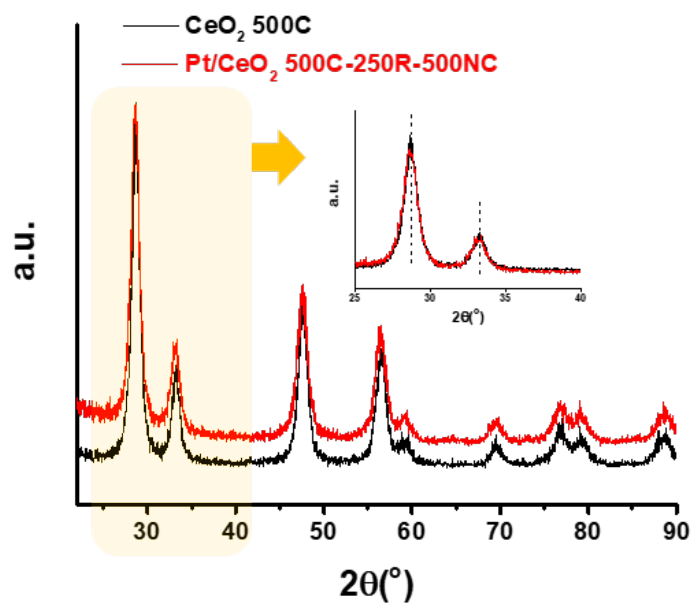


Fig. S13 XRD patterns of CeO₂ 500C and Pt/CeO₂ 500C-250R-500NC. CeO₂ aggregation was not promoted on Pt/CeO₂ 500C-250R by the 500NC treatment.

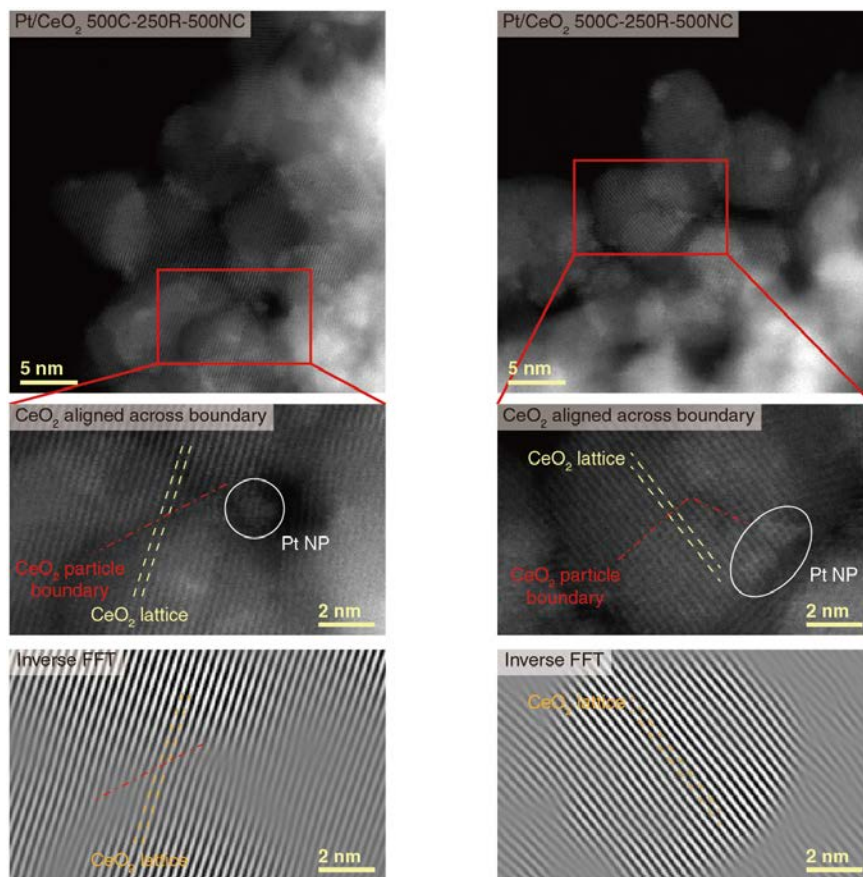


Fig. S14 Representative HAADF-STEM images of Pt/CeO₂ 500C-250R-500NC. The CeO₂ particles with the aligned lattice are marked with the red square. Some of Pt NPs (1~2 nm in diameter) formed by 500NC treatment are also marked with the white circle.

Supplementary References

1. W. C. Lee, B. H. Kim, S. Choi, S. Takeuchi and J. Park, *J. Phys. Chem. Lett.*, 2017, **8**, 647-654.